Caveolin Scaffolding Region and the Membrane Binding Region of Src Form Lateral Membrane Domains†

Stephen P. Wanaski, Benjamin K. Ng, and Michael Glaser*

Department of Biochemistry, University of Illinois, Urbana, Illinois 61801

Received November 27, 2001; Revised Manuscript Received November 1, 2002

ABSTRACT: Formation of domains by the membrane binding motifs of caveolin and src were studied in large unilamellar vesicles using fluorescence digital imaging microscopy. Caveolin, a major structural protein of caveolae, contains a scaffolding region (residues 82−101) that contributes to the binding of the protein to the plasma membrane. A caveolin peptide (82−101) corresponding to this scaffolding region induced the formation of membrane domains enriched in the acidic lipids phosphatidylserine and phosphatidylinositol-4,5-bisphosphate. Cholesterol, another predominant component of caveolae, was also enriched in these domains. Caveolae also contain many different signaling molecules including src family tyrosine kinases. Src proteins bind to the plasma membrane via a N-terminal myristate chain and a cluster of basic residues that can interact electrostatically with negatively charged lipids. A peptide corresponding to the src membrane binding motifs (residues myr-2−19) sequestered acidic lipids into lateral membrane domains. Both the src and the caveolin peptides colocalized together with acidic lipids in the domains. Control experiments show the domains are not the result of vesicle aggregation. Two-photon fluorescence correlation spectroscopy experiments suggest diffusion in the domains was slower, but the domains were dynamic. Protein kinase C phosphorylated src in its N-terminal membrane binding region; however, the caveolin scaffolding peptide inhibited this activity. Consequently, protein-induced membrane domains may affect cell signaling by organizing signal transduction components within the membrane and changing reaction rates.

The plasma membrane of cells is a dynamic, heterogeneous mixture of proteins and lipids. The organization of signaling molecules into discrete membrane domains can provide a new level for the regulation and specificity of numerous cell signaling pathways. Lateral membrane domains may serve to concentrate components in a localized area, increasing enzyme activity and facilitating protein interactions. For instance, in the calcium−phospholipid second messenger system, protein kinase C (PKC)[1] was shown to be most active when all of its coactivators were localized into membrane domains along with the substrate and the enzyme (*1*). Peptides corresponding to the membrane binding region of MARCKS, the major PKC substrate in most cell types, was shown to form domains enriched in acidic lipids PS and PIP_2 (*2*). The sequestering of the lipid signaling molecule PIP_2 into domains by the MARCKS peptide was shown to inhibit phospholipase C activity—a functional consequence of the membrane organization of proteins and lipids in domains (*2*). The molecular mechanism of domain formation includes the interaction of basic stretches of amino acids binding to acidic lipids through nonspecific electrostatic interactions to minimize the free energy of the system (*3*). However, insertion of hydrophobic residues into the membrane may also play a role in forming membrane domains. Fluorescence digital imaging microscopy allows for the direct visualization of these interactions along with quantifying membrane components in the domains (*4*−*7*).

Caveolae are small (50−100 nm), specialized regions in the plasma membrane of most cell types (for reviews, see refs *8*−*11*). Caveolae can bud from the plasma membrane and function in cellular processes such as endocytosis and the transcytosis of molecules (*12*, *13*). The membrane is recycled, and this activity is dependent upon PKCα activity (*14*). These distinct membrane domains are enriched in numerous signaling molecules including platelet-derived growth factor receptors, phosphatidylinositol-3 kinase, src tyrosine kinases, PKC, PLC, and PIP_2 (*15*, *16*). Caveolae also have a unique lipid composition containing high concentrations of cholesterol and sphingolipids (*17*−*19*) thought to alter the phase of caveolae membranes from a liquid crystalline to a liquid-ordered state, and consequently, to confer resistance to extraction by detergents (*20*−*22*). These detergent-resistant domains have been found in cells that do not contain caveolin. Current theories of caveolae formation include derivation from lipid rafts or from caveolae-related domains that form because of high cholesterol and high glyco- and

† This work was supported in part by National Institutes of Health Grant GM 54144 and Multiple Sclerosis Society Grant RG 2660.

* To whom correspondence should be addressed. Tel: (217) 333-3960. Fax: (217) 244-5858. E-mail: m-glaser@uiuc.edu.

[1] Abbreviations: DAG, diacylglycerol; dansyl, 5-(dimethylamino)-naphthalene-1-sulfonyl; DOPC, dioleylphosphatidylcholine; DOPS, dioleylphosphatidylserine; DTT, dithiothreitol; DUA, dansylundecanoic acid; FCS, fluorescence correlation spectroscopy; MARCKS, myristoylated alanine-rich C kinase substrate; MOPS, 3-(n-morpholino)propanesulfonic acid; NBD, 7-nitrobenz-2-oxa-1,3-diazol-4-yl; PC, phosphatidylcholine; PDGF, platelet-derived growth factor; PIP_2, phosphatidylinositol-4,5-bisphosphate; PKC, protein kinase C; PLC, phospholipase C; PS, phosphatidylserine.

10.1021/bi012097n CCC: $25.00
Published on Web 12/10/2002

sphingolipid contents in the membrane. These rafts or domains then form caveolae upon expression of the caveolae marker protein caveolin (for a review, see ref *23*).

The caveolin protein is a 22 kDa integral membrane protein thought to play structural and functional roles in caveolae. Caveolae are thought to form because of the oligomerization of caveolin, the major structural protein of caveolae (*24*−*26*). These proteins contain a scaffolding region (residues 82−101) just upstream of its membrane spanning domain that is both necessary and sufficient for caveolin membrane binding (*27*). This scaffolding region contains basic residues that can bind to acidic lipids in the membrane such as PS and PIP_2 through nonspecific electrostatic interactions (*28*). The region also contains seven hydrophobic residues that may penetrate the bilayer and aid in membrane binding (*29*).

We propose that the formation of caveolae involves the caveolin scaffolding region binding to membranes and forming lateral domains enriched in acidic lipids and cholesterol. This seems reasonable given this peptide's hydrophobic character and specificity for acidic lipids, along with its close proximity to the membrane in the intact protein. This mechanism may help to explain the localization of other signaling molecules in caveolae such as src. Src is a nonreceptor tyrosine kinase that binds to the plasma membrane via insertion of an N-terminal myristate anchor and a cluster of basic residues interacting electrostatically with acidic lipids in the membrane (*30*). The N-terminal region of src contains phosphorylation sites for protein kinase C and cAMP-dependent protein kinase (*31*). Phosphorylation at these sites weakens src binding affinity for membranes and may displace the protein from the plasma membrane (*32*−*34*). A number of recent papers have addressed the general mechanisms of how proteins can induce the formation of membrane domains (*35*−*43*).

In this paper, lateral organization of the caveolin scaffolding region in synthetic phospholipid vesicles containing acidic lipids and cholesterol was investigated. Localization of the N-terminal membrane binding region of src was also studied in vesicles containing acidic lipids. The colocalization of src and caveolin peptides into membrane domains leads to the inhibition of PKC phosphorylation, and this can serve as a general model for how the caveolin scaffolding region acts as an inhibitor of signal transduction (*10*).

MATERIALS AND METHODS

Materials. The lipids DOPC, lyso-PC, DOPS, NBD-PS, and DAG were purchased from Avanti Polar Lipids, Inc. (Alabaster, AL). Cholesterol and gramicidin were obtained from Sigma Chemical Co. (St. Louis, MO). NBD-cholesterol, tetramethyl-rhodamine iodoacetamide (TMRIA), dansylundecanoic acid, and dansyl chloride were obtained from Molecular Probes (Eugene, OR). PIP_2 was purchased from Calbiochem (La Jolla, CA). NBD-PIP_2 was a gift from Dr. Glen Prestwhich. γ-^{32}P-ATP was obtained from Amersham Pharmacia Biotech, Inc. (Piscataway, NJ). The caveolin scaffolding region peptide (residues 82−101; H-CGIWKASFTTFTVTKYWFYR-NH_2) and the peptide corresponding to the N-terminus of src (myr-2−19, C; myristate-GSSKSKPKDPSQRRRSLEC) were obtained from Dr. Stuart McLaughlin and were also synthesized by the Biotechnology Center at the University of Illinois at Urbana-Champaign. *Spodoptera frugiperda* (Sf9) cells were obtained from American Type Culture Collection (No. CRL-1711). The PKCα baculovirus construct was obtained from Drs. Peter Parker and Julianne Sando.

Preparation of Large Unilamellar Vesicles for Fluorescence Digital Imaging Microscopy. Large unilamellar vesicles for microscopy were prepared using the method employed by Haverstick and Glaser (*44*). Typically, 250 nmol of lipid in chloroform was mixed in a small (15 × 45 mm) glass vial. The mixture was dried under nitrogen leaving a thin, uniform layer of lipid on the glass. The vials were placed under vacuum at room temperature in the dark for 24 h. The lipid was hydrated slowly at 37 °C overnight in 500 μL of a buffer solution. Alternatively, large unilamellar vesicles were formed according to Needham and Evans (*45*). Circular Teflon disks with a 0.9-mm radius were made to fit inside a 5 mL beaker. The disks were roughened on one side with fine sandpaper, cleaned, and washed in chloroform. Typically, 250 nmol of lipid was dried under a gentle stream of nitrogen on top of the roughened Teflon disks. The disks were placed into 5-mL beakers (lipid film facing up) and left under vacuum for 24 h in the dark. The vesicles were then formed by the addition of 500 μL of a buffer solution at 37 °C overnight.

Synthesis of Large Unilamellar Vesicles Containing the Caveolin Peptide (82−101, C) for Fluorescence Digital Imaging Microscopy. Because the caveolin peptide (82−101, C) is very hydrophobic, it was dissolved in methanol and added at appropriate concentrations to 250 nmol of lipid (in chloroform). The mixture was dried down under nitrogen gas in a small glass vial (15 × 45 mm) to form a smooth, thin film on the glass. The vials were placed under vacuum for 24 h and hydrated slowly in 500 μL of a buffer solution at 37 °C overnight.

Synthesis of Dansyl-Labeled Phosphatidylcholine (DUA-PC). Synthesis of DUA-PC from dansylundecanoic acid and lyso-PC was performed according to Gupta et al. (*46*). Fatty acyl anhydride formation: 50 mg dansylundecanoic acid was mixed with 23.7 mg dicyclohexylcarbodiimide (equimolar amounts) in 2.0 mL of chloroform. This solution was stirred in the dark for 2 h and then filtered through a glass wool column. The solvent was removed using a rotary evaporator. Concurrently, 40.2 mg lyso-PC and 9.45 mg dimethylaminopyridine (equimolar amounts) were dried together in toluene under N_2. The fatty acyl anhydride was dissolved in 3.3 mL of chloroform to achieve a 1.5 molar excess of fluorescent fatty acid to lyso-PC. The dissolved solution was added to the dried lyso-PC and reacted overnight under N_2, with shaking in the dark. The reaction mixture was dried under N_2 to 0.5 mL volume, spotted on a preparative thin-layer chromatography plate (silica gel G), and resolved in chloroform/methanol/H_2O (65:25:4). The band corresponding to DUA-PC was scraped and eluted from the silica with chloroform/methanol/H_2O/concentrated HCl (50:100:5:0.5). The solution was dried to a volume of 1.6 mL, and the product was extracted according to the procedure of Bligh and Dyer (*47*). DUA-PC was quantitated by phosphate analysis (*48*) using the absorbance of dansyl as $\epsilon_{335nm} = 4800$ M^{-1} cm^{-1}.

Synthesis of Dansyl-Labeled Phosphatidylserine from Dansyl-Labeled Phosphatidylcholine. The reaction was

performed as described by Comfurious et al. (*49*) and Luan and Glaser (*6*). Briefly, 200 μmol of DUA-PC was dried under N_2. To this, 2.0 mL of a 50% L-serine and 2% octylglucoside in 100 mM $CaCl_2$ and 100 mM sodium acetate solution was added and stirred vigorously at 45 °C for 10 min. The synthesis was done enzymatically by addition of 10 μL of a 1 mg/mL solution of phospholipase D (from *Streptomyces species*) and incubated at 45 °C with gentle shaking. After 1.5 h, another 10 μL of enzyme solution was added and incubated for another 1.5 h at 45 °C. The reaction was stopped by addition of 1.0 mL of 0.05 M EDTA (pH = 8.0). Five volumes of methanol were added, and the mixture was shaken. Five volumes of $CHCl_3$ were added and shaken again. The mixture was centrifuged, and the aqueous layer was discarded. The lipid was purified by thin-layer chromatography and quantitated as was done for the synthesis of DUA-PC.

Preparation of Small, Unilamellar, Extruded Vesicles for Use in Protein Kinase C Activity Assays. Small unilamellar vesicles (100 nm diameter) were formed using a LiposoFast lipid extruder from Avestin, Inc. (Ontario, Canada). A concentrated lipid mixture (>2 μmol total lipid) was dried under N_2 and placed under vacuum for 24 h. The lipid was hydrated in 0.5 mL of a buffer solution and vortexed vigorously for 1.0 min. The solution was then passed through 100 nm-pore polycarbonate membrane filters 25 times.

Expression and Purification of PKCα *from Sf9 Cells.* Baculovirus expression and purification of PKCα was performed as by Stabel et al. (*50*) with slight alterations. After 4 days (peak of PKC expression), cells were harvested and extracted in 25 mL of buffer A (20 mM Tris-HCl (pH 7.5), 5 mM EDTA, 10 mM benzamidine, 0.3% (v/v) 2-mercaptoethanol, and 0.5% (v/v) Triton X-100) plus 50 μg/mL PMSF and 10 ug/mL leupeptin. The solution was centrifuged in an ultracentrifuge at 40 000*g* for 25 min. The supernatant was loaded onto a Sephacryl S-200HR column (5 × 60 cm) and run in buffer B (buffer A with Triton X-100 reduced to 0.02% (v/v)). The PKCα pool was loaded onto a DEAE-cellulose column (75 mL) equilibrated with buffer B. Protein was eluted at 0.5 mL/min with buffer B and 150 mM NaCl. The active pool was adjusted to 1.0 M salt by slow addition of NaCl at 4 °C and then loaded onto a phenyl-sepharose column (0.9 × 22 cm) equilibrated in buffer B and 1.0 M NaCl. The column was washed with 3× volumes of buffer B and 1.0 M NaCl at 0.75 mL/min. Protein was eluted with 200 mL of a negative salt gradient of buffer B and 1.0 M NaCl to buffer B alone and then washed with an additional 100 mL of buffer B. The purified protein was dialyzed into buffer B and 25% glycerol, quantitated by the BCA protein assay (Sigma), and stored at −80 °C.

Protein Kinase Activity Assays. The assay for PKC activity was performed by measuring the incorporation of ^{32}P from [γ-^{32}P]ATP into the MARCKS or src peptides as described by Chakravarthy et al. (*51*), Edashige et al. (*52*), and Yang and Glaser (*7*). The reaction typically contained 0.1 mM lipid vesicles (extruded vesicles or mixed micelles), 10 mM $MgCl_2$, 0.3 mM $CaCl_2$, 50 μM ATP, 0.25 μCi of [γ-^{32}P]-ATP, 6 μM MARCKS or src peptides, and 0.5−2.0 μg of PKCα in 10 mM Tris, pH 7.0. The final volume was 200 μL. The reaction was incubated for 20 min at room temperature and stopped by addition of 100 μL of ice-cold 10% trichloroacetic acid. Samples were incubated on ice for 30 min, then filtered and washed with ice-cold 10% trichloroacetic acid on 2.0 cm^2 GF/C glass filters. Filters were placed and dried in glass scintillation vials and suspended in scintillation fluid (0.3% PPO and 25% Triton X-114 in xylene). ^{32}P was counted using a Beckman LS7000 scintillation counter.

Fluorescence Digital Imaging Microscopy. Studies of the lateral organization of proteins and lipids in large unilamellar vesicles were performed as by Haverstick and Glaser (*44*) and Yang and Glaser (*1*). Image processing and quantitation was described in Yang and Glaser (*1*). The maximum enrichment of a lipid in a vesicle is defined as being equal to the highest radiance value for a pixel in the domain, for example, a subsection of a domain/(the lowest radiance value for a pixel in the vesicle)(highest/lowest radiance values for the vesicles in the absence of a peptide). This parameter reflects the total range of concentrations observed for a lipid in the vesicles because of domain formation caused by the peptide.

Fluorescence Correlation Spectroscopy (FCS) Experiments. The instrumentation and processing for two-photon excitation fluorescence correlation spectroscopy is described in refs *53* and *54* with some modifications. Experiments were carried out on a Zeiss Axiovert 135 TV microscope (Thornwood, NY) with a 63X oil immersion objective (NA = 1.2). Excitation of the sample was between 770 and 780 nm. Samples were prepared as described previously for fluorescence digital imaging microscopy experiments. Vesicles were composed of 90 mol % DOPC, 10 mol % DOPS or 67 mol % DOPC, and 33 mol % DOPS hydrated in 0.5 mM MOPS buffer, pH 7.4. Data analysis was performed using PV-WAVE (Visual Numerics) and Origin (Microcal Software, Inc.).

RESULTS

Peptide Corresponding to the Caveolin Scaffolding Region Forms Lateral Membrane Domains Enriched in Acidic Lipids and Cholesterol. Fluorescence digital imaging microscopy was used to visualize the lateral distribution of lipids in large unilamellar vesicles upon the addition of a peptide corresponding to the caveolin scaffolding region. Vesicles composed of 89 mol % DOPC, 9.5 mol % DOPS, 1 mol % PIP_2, and 0.5 mol % NBD-PS in 1 mM MOPS, 100 mM KCl, and 2 mM DTT (pH 7.0) showed a uniform dispersion of NBD-labeled phosphatidylserine (Figure 1A, upper images). Addition of 40 μM caveolin scaffolding region (residues 82−101) to vesicles of the same composition induced the formation of membrane domains enriched in NBD-PS (Figure 1A, lower images). These images represent three different vesicles taken from a population that contained domains induced by the caveolin peptide (82−101). To view the localization of the signaling molecule PIP_2, vesicles composed of 89 mol % DOPC, 10 mol % DOPS, 0.5 mol % PIP_2, and 0.5 mol % NBD-PIP_2 in 1 mM MOPS, 100 mM KCl, and 2 mM DTT (pH 7.0) were constructed. Prior to the addition of the caveolin peptide (82−101), there was a uniform distribution of NBD-PIP_2 in these vesicles as viewed for NBD-PIP_2 fluorescence (Figure 1B, upper images). PIP_2 was sequestered into lateral membrane domains in the presence of 40 μM caveolin peptide (Figure 1B, lower images).

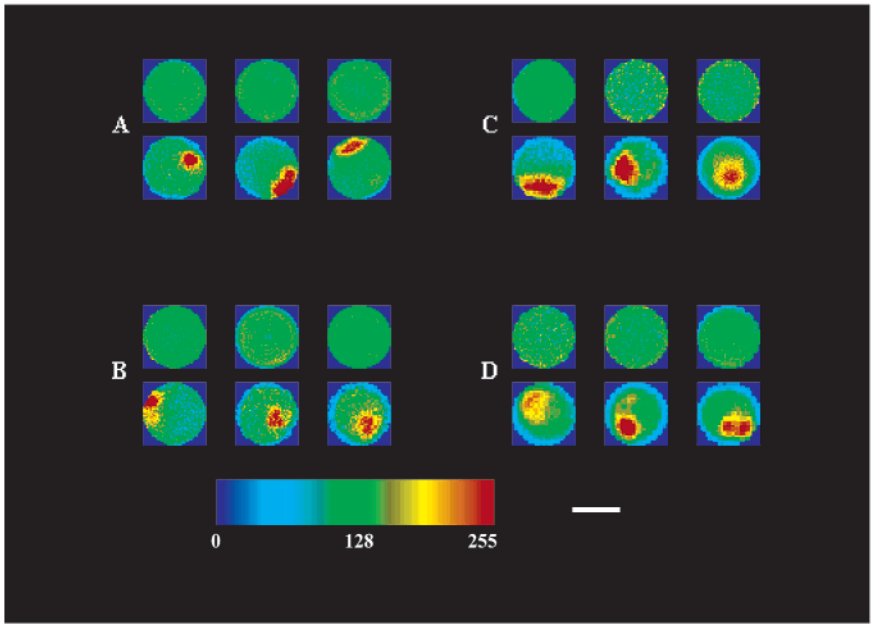

FIGURE 1: Caveolin peptide (82−101) forms domains enriched in PS, PIP_2, and cholesterol. (A) Vesicles composed of 89 mol % DOPC, 9.5 mol % DOPS, 1 mol % PIP_2, and 0.5 mol % NBD-PS displayed a uniform distribution of PS in 1 mM MOPS, 100 mM KCl, 2 mM DTT, pH 7.0 (upper images). Addition of 40 μM caveolin (82−101) peptide induced the formation of domains enriched in NBD-PS (A, lower images). Vesicles of the same composition as in A (89 mol % DOPC, 10 mol % DOPS, 0.5 mol % PIP_2, and 0.5 mol % NBD-PIP_2) but viewed for NBD-PIP_2 fluorescence had a random distribution of PIP_2 in the absence of caveolin peptide (B, upper images). PIP_2 was localized into domains induced by addition of 40 μM caveolin peptide (B, lower images). (C) Vesicles containing 57 mol % DOPC, 32.5 mol % DOPS, 10 mol % cholesterol, and 0.5 mol % NBD-PS had a uniform distribution of PS in the absence of caveolin peptide (C, upper images) and a clustering of PS in the presence of caveolin peptide (C, lower images). Vesicle images in D are of the same composition as in C, however, they are viewed for NBD-cholesterol (57 mol % DOPC, 33 mol % DOPS, 9.5 mol % cholesterol, and 0.5 mol % NBD-cholesterol). Cholesterol was distributed randomly prior to the addition of 40 μM caveolin but was heterogeneous in the presence of peptide (D, lower images). All images were normalized to a mean radiance value of 100 ± 5, and the corresponding intensity values are displayed using the pseudo-color scheme at the bottom of the figure. The white bar equals 4 μm.

Since caveolae have been shown to have high concentrations of cholesterol, we next studied the caveolin peptide (82−101) binding to vesicles containing acidic lipids and cholesterol (*15*). Vesicles composed of 57 mol % DOPC, 32.5 mol % DOPS, 10 mol % cholesterol, and 0.5 mol % NBD-PS in 1 mM MOPS, 100 mM KCl, and 2 mM DTT (pH 7.0) displayed a uniform distribution of PS prior to the addition of the caveolin peptide (Figure 1C, upper images). The lower panel in Figure 1C shows the formation of domains enriched in NBD-PS induced by 40 μM caveolin peptide in vesicles containing cholesterol. The images in Figure 1D are viewed for NBD-cholesterol fluorescence, and this fluorophore was randomly distributed in the vesicles prior to adding the caveolin peptide (upper images). Cholesterol was also localized into domains induced by the caveolin peptide. It is common for the content of PS to be 10% in the plasma membrane of a cell or higher (*55*). If PS is located mainly in the inner leaflet of the plasma membrane, then the PS content is doubled to 20% or higher. In addition, there may be a range of PS concentrations in biological membranes because of the formation of domains. Consequently, a number of different lipid compositions have been used in the present studies to demonstrate that domains can be formed under a variety of conditions.

Enrichment of Lipid Molecules Induced by the Caveolin Peptide (82−101). Compositional analysis of the domains induced by the caveolin peptide was performed as by Luan et al. (*56*) and Yang and Glaser (*7*). The images in Figure 1 represent data taken from a population of 35−50 vesicles. Figure 2A shows the maximum enrichment (equal to [the highest radiance value for a pixel in the domain, i.e., a subsection of a domain]/[(the lowest radiance value for a pixel in the vesicle)(highest/lowest radiance values for the vesicles in the absence of a peptide)]) of both NBD-PS and NBD-PIP_2 in vesicles corresponding to the conditions in Figure 1A,B. The maximum enrichment reflects the total range of concentrations observed for a lipid in the vesicles because of domain formation caused by the peptide. Addition of the caveolin peptide induced domains that showed a 5-fold range of PS concentrations. PIP_2 was enriched 7-fold in these vesicles. The area of the vesicle occupied by a domain is arbitrarily defined as the fluorescence intensity that is 1.5 times greater than the mean fluorescence intensity of the vesicle (*7*). Figure 2B shows the area of domains in the vesicle population. The average domain area induced by addition of caveolin (82−101) was 13% for those enriched in PS and 10% for those enriched in PIP_2 as opposed to 0.5 and 1% for the control conditions, respectively. Using the same quantitation methods, cholesterol had a 4-fold maximum enrichment induced by addition of the caveolin peptide (Figure 2C, corresponding to the vesicle images in Figure 1D). Similarly, the average area of these domains enriched in cholesterol was 17% for the vesicles in the population. The error in the enrichment and area measurements was calculated as the standard deviation of the mean between populations of the vesicle samples under each set of experimental conditions ($n = 3$).

N-terminal Src Peptide Forms Domains Enriched in Acidic Lipids and Colocalizes with the Caveolin Scaffolding Region (82−101). Membrane association of src is required for proper

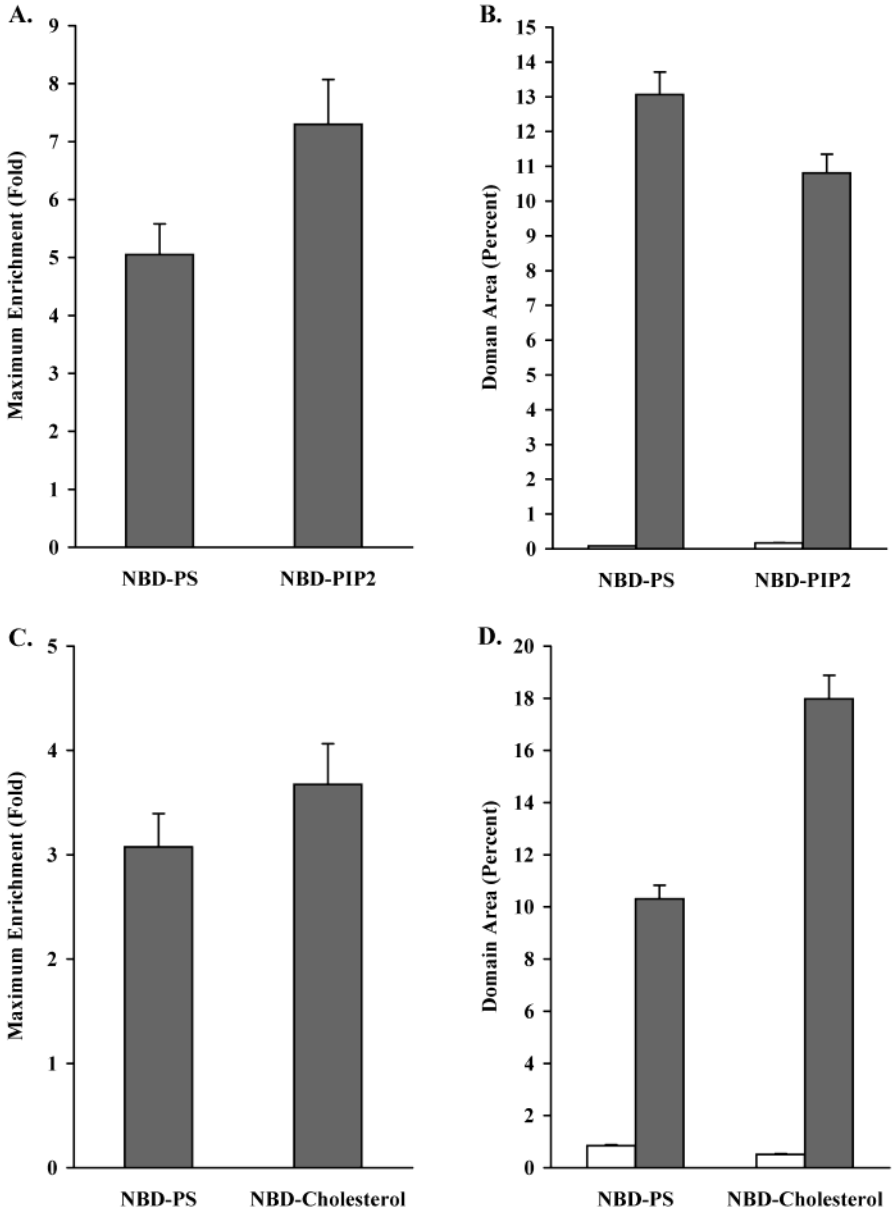

FIGURE 2: Acidic lipids and cholesterol are highly enriched in lateral membrane domains induced by caveolin (82−101). The maximum enrichments of PS and PIP_2 for a population of vesicles from Figure 1A,B upon addition of 40 μM caveolin peptide are given in Figure 2A, and the areas of the vesicles enriched in PS or PIP_2 are given in Figure 2B. The maximum enrichments of PS and cholesterol for a population of vesicles from Figure 1C,D in the presence of 40 μM caveolin peptide are given in Figure 2C, and the domain areas of the vesicles enriched in PS and cholesterol are given in Figure 2D. The open bars are the areas of domains in vesicles in the absence of the peptide, and the solid bars are the areas of domains in the presence of the peptide.

cell function; src binds to membranes through its N-terminal myristate chain and through a stretch of basic amino acids that interact electrostatically with acidic lipids (*30*). Fluorescence digital imaging microscopy was used to view the localization of peptides corresponding to the membrane binding motif of src in vesicles containing acidic lipids. Both caveolin (82−101) and src (myr-2−19, C) induced the formation of domains enriched in phosphatidylserine when added to vesicles containing 33% acidic lipid (Figure 3B,C, respectively). Addition of 20 μM caveolin peptide induced a 4-fold enrichment in PS, while 3 μM src peptide induced a 7-fold enrichment in PS (Figure 4A). The average area of domains formed by the addition of these peptides was 8 and 14% for caveolin and src, respectively (Figure 4B). Adding both peptides to vesicles containing 33% acidic lipid induced domains similar to those in enrichment and area as with the src peptide alone (Figures 3D and 4A,B). To show the colocalization of both caveolin (82−101) and src (myr-2−19, C) in membrane domains, rhodamine-labeled caveolin and acrylodan-labeled src peptides were incubated with unlabeled vesicles of the same composition. Acrylodan-labeled src peptides were localized to discrete regions of the vesicle membrane (Figure 3E, upper images). Rhodamine-labeled caveolin was localized to the same domains when the vesicles were viewed for rhodamine fluorescence (Figure 3E, lower images). The domains shown in Figures 1 and 3 formed because of the addition of caveolin and src peptides and not because of vesicle aggregation. The total NBD fluorescence intensities were not affected by the addition of these peptides to the vesicles; while the enrichments of the

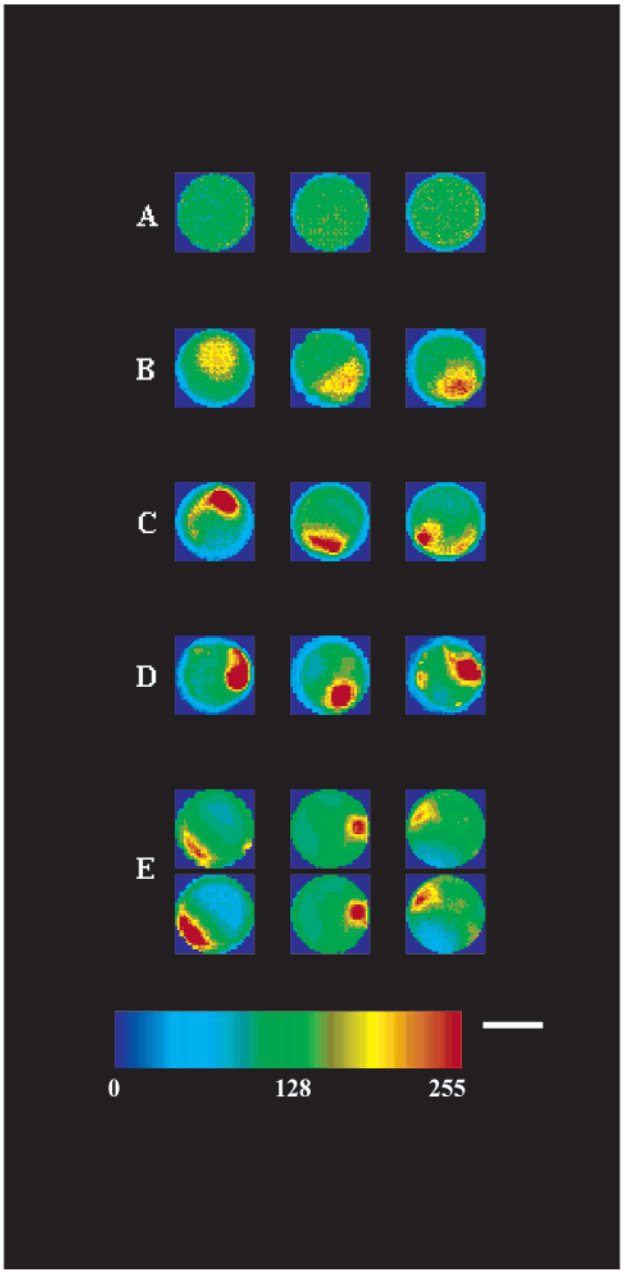

FIGURE 3: Caveolin (82−101) and src (myr-2−19, C) peptides induce the formation of membrane domains enriched in PS, and they colocalize. (A) Vesicles composed of 50 mol % DOPC, 32.5 mol % DOPS, 10 mol % cholesterol, 5 mol % DAG, 2 mol % PIP_2, and 0.5 mol % NBD-PS in 10 mM MOPS and 100 mM KCl (pH 7.0) displayed a uniform distribution of PS prior to the addition of src or caveolin. (B) Addition of 20 μM caveolin scaffolding domain peptide induced the formation of domains enriched in PS. (C) Addition of 3 μM src peptide induced the formation of domains enriched in PS. Phosphatidylserine was highly enriched in domains in the presence of both 3 μM src peptide and 20 μM caveolin peptide (D). Addition of 3 μM acrylodan-labeled src peptide and 20 μM rhodamine-labeled caveolin peptide to unlabeled vesicles of the same composition as in A showed the two peptides localized in the same membrane domains. Upper images in E are viewed for acrylodan-src (myr-2−19, C) fluorescence, and the lower images in E are viewed for rhodamine-caveolin (82−101) fluorescence. All images were normalized to a mean radiance value of 100 ± 5, and the corresponding intensity values are displayed using the pseudo-color scheme at the bottom of the figure. The white bar equals 4 μm.

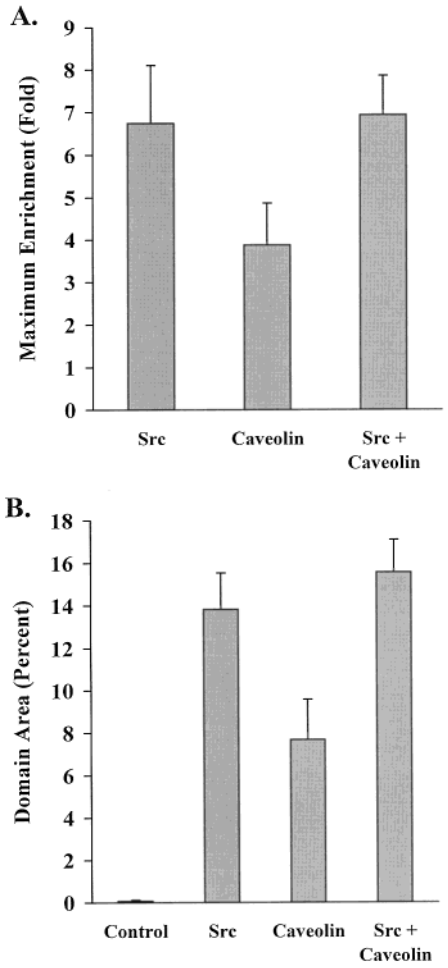

FIGURE 4: Phosphatidylserine is highly enriched in domains induced by both caveolin (82−101) and src (myr-2−19, C). (A) Maximum enrichments of phosphatidylserine were calculated from a population of vesicles displayed in Figure 3A−D. (B) The domain areas of the vesicles enriched in PS.

lipid and peptide species in domains increased upon addition of the peptides to the vesicles, there was no increase in the total fluorescence intensity of NBD-PS (data not shown). Also, there was little, if any, energy transfer between acrylodan and rhodamine under these experimental conditions (data not shown).

Caveolin Scaffolding Region (82−101) Inhibits Protein Kinase C Phosphorylation of N-terminal Src Peptide. Protein kinase C activity assays were performed using src (myr-2−19, C) as a substrate bound to extruded vesicles (100 nm) containing acidic lipids. Diacylglycerol was added (5 mol %) to these vesicles to activate PKC. PKC phosphorylates the N-terminal src peptide on serine residue 12 (*31*), while the caveolin peptide is not a substrate for PKC. In the absence of caveolin (82−101), PKC readily phosphorylated the src peptide at both low and high salt concentrations, with PKC being more active under the low salt conditions (Figure 5), consistent with data obtained with the MARCKS peptide by Yang and Glaser (*7*). Upon addition of a 10 μM caveolin scaffolding region peptide, PKC activity was inhibited at both salt concentrations (each salt condition normalized separately in Figure 5). At low salt (1 mM MOPS, 50 μM ATP, 0.1 mM extruded vesicles, 10 mM $MgCl_2$, 0.3 mM $CaCl_2$, 6 μM src peptide, and 0.25 mCi γ-^{32}ATP, pH 7.0), the PKC phosphorylation of src was reduced to approximately 5% in the presence of 20 μM caveolin scaffolding peptide. At the high salt condition (addition of 100 mM KCl) where domains

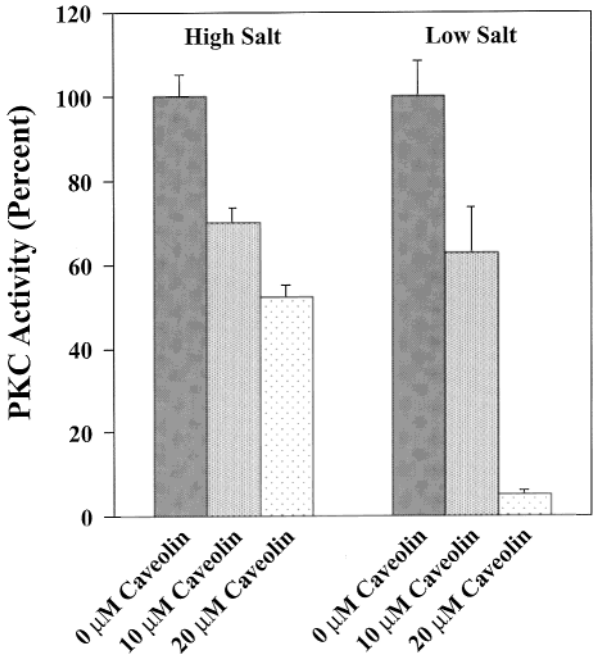

FIGURE 5: Caveolin scaffolding region inhibits PKC phosphorylation of the N-terminal src peptide. PKC activity assays were performed using 6 μM src (myr-2−19, C) as a substrate bound to 0.1 mM vesicles (51 mol % DOPC, 33 mol % DOPS, 10 mol % cholesterol, 5 mol % DAG, and 1 mol % PIP_2) in 1 mM MOPS and 100 mM KCl, pH 7.0 (high salt), or 1 mM MOPS, pH 7.0 (low salt). The assay mixture contained 50 μM ATP, 10 mM $MgCl_2$, 300 μM $CaCl_2$, and 0.25 μCi γ^{32}P-ATP. 100 mM KCl was added to the assay mixture for the high salt conditions.

were not as enriched, the PKC phosphorylation of src was approximately 50% of the control in the presence of 20 μM caveolin peptide, suggesting a strong electrostatic effect.

Formation of Lateral Membrane Domains Induced by Caveolin (82−101) and Src (myr-2−19, C) Are Enriched in PS, not PC. To demonstrate that the formation of membrane domains induced by the src and caveolin peptides was not a result of vesicle aggregation, a series of experiments were carried out. A direct way to demonstrate that aggregation cannot account for the results is to add the peptides to vesicles containing fluorescent labels on both PS and PC simultaneously. Figure 6A,B,C shows vesicles composed of 64% DOPC, 32.7% DOPS, 3% dansyl-labeled PC, and 0.3% NBD-labeled PS in 10 mM Tris buffer, pH 7.0. Prior to the addition of peptides, there was a uniform distribution of both NBD-labeled PS (Figure 6A, upper images) and dansyl-labeled PC (6A, lower images) in the vesicles. Addition of 20 μM caveolin peptide (82−101) induced the formation of PS domains (Figure 6B, upper panel); however, the distribution of dansyl-labeled PC was uniform (Figure 6B, lower panel). Similarly, addition of 3 μM src peptide (myr-2−19, C) caused a clustering of PS into domains (Figure 6C, upper images), while dansyl-PC remained homogeneous (Figure 6C, lower images).

Switching the two fluorophores on PS and PC provides a good control to show that the fluorophores themselves are not influencing the results. Figure 6D,E,F shows vesicles composed of 66.7% DOPC, 30% DOPS, 3% dansyl-labeled PS, and 0.3% NBD-labeled PC in 10 mM Tris buffer, pH 7.0. The upper images in these panels are viewed for NBD-PC fluorescence, and the lower images are viewed for dansyl-PS fluorescence. Both displayed a random mixing prior to the addition of peptide (Figure 6D). The upper panel in Figure 6E showed the uniform distribution of PC upon addition of 20 μM caveolin (82−101), while the lower images showed a clustering of dansyl-labeled PS induced by caveolin. The same effect was seen after addition of the 3 μM src peptide—a uniform array of NBD-PC (Figure 6F, upper panel) and domains enriched in dansyl-PS (Figure 6F, lower images).

Gramicidin Does Not Localize in Domains Induced by the Src Peptide (myr-2−19, C). Gramicidin is a polypeptide ionophore that inserts completely into a bilayer. Since it does not demonstrate any affinity for a specific phospholipid and it is readily available, it has been used to represent a typical protein that would not necessarily be concentrated in a domain (e.g., refs *56*, *57*). Large unilamellar vesicles were constructed containing 67% PC, 32.7% PS, 0.3% NBD-PS, and 20 μM dansyl-labeled gramicidin for study using fluorescence digital imaging microscopy. The upper images in Figure 7A show a uniform distribution of NBD-PS before src (myr-2−19, C) was added. The lower images in Figure 7A correspond to the same three vesicles viewed for dansyl-gramicidin fluorescence, also randomly distributed. Addition of 3 μM src peptide induced the formation of NBS-PS domains (Figure 7B, upper panel); however, dansyl-gramicidin was not enriched in the domains (Figure 7B, lower panel) and behaved in a manner similar to PC.

Formation of Lateral Membrane Domains Enriched in PS Induced by the N-terminal Src Peptide in the Presence of Vesicles Labeled with Another Fluorophore Do Not Show Aggregation. Another way to examine if aggregation occurs at the site of domain formation is to mix vesicles that have been labeled with either NBD-PS or dansyl-PS. Figure 8A shows images of such vesicles (from an equimolar mixture) after the addition of the src peptide. The images on the left reflect dansyl fluorescence, and the top two vesicles show domains enriched in dansyl-PS (presumably derived from vesicles labeled only with dansyl-PS). They had no NBD fluorescence above background (right images). Conversely, vesicles that had domains enriched with NBD-PS (i.e., the two bottom vesicles, presumably derived from vesicles labeled only with NBD-PS) showed no dansyl fluorescence, clearly indicating the absence of aggregation. A total of 60 vesicles was examined (30 corresponding to the top two vesicles and 30 corresponding to the bottom two vesicles), and in no case was there significant fluorescence because of the second fluorophore.

It is theoretically possible that the large vesicles fragmented into smaller vesicles when the peptide was added and that the small vesicles could aggregate on the larger vesicle and give the appearance of domains (*58*). The fragmented small vesicles would have to be smaller than the limit of resolution of the microscope since they are not visible when the larger vesicles are examined. To further test this idea with highly favorable conditions for aggregation, 0.1 mM small, extruded vesicles (100 nm) containing 67% PC, 30% PS, and 3.0% dansyl-labeled PS were added to 0.1 mM large unilamellar vesicles of the same composition but labeled with NBD-PS (67% PC, 32.7% PS, and 0.3% NBD-PS). The small vesicles are below the resolution limit of the microscope. There was a uniform distribution of lipid in the large unilamellar vesicles (viewed for NBD-PS fluorescence) before src was added (Figure 8B), and there was no

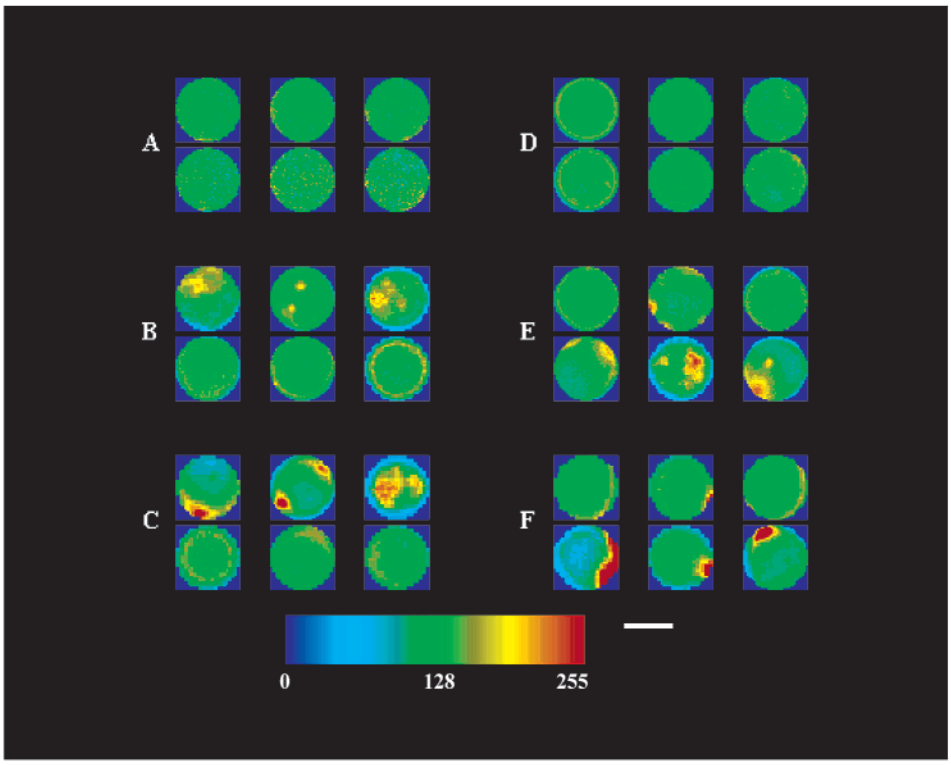

FIGURE 6: Caveolin and src peptides form domains enriched in PS, not PC. Vesicles composed of 64 mol % DOPC, 32.7 mol % DOPS, 3 mol % dansyl-PC, and 0.3 mol % NBD-PS in 10 mM Tris buffer (pH 7.0) had a uniform distribution of lipid prior to the addition of peptide (A). The upper images in A are viewed for NBD-PS fluorescence, and the lower images are the same three vesicles viewed for dansyl-PC fluorescence. Domains enriched in PS formed in the presence of 20 μM caveolin peptide (B, upper images); however, dansyl-PC remained uniformly distributed in the vesicles (B, lower images). Addition of 3 μM src peptide caused a clustering of PS (C, upper images), but the localization of dansyl-PC remained uniform in the vesicles (C, lower images). Vesicles composed of 66.7 mol % DOPC, 30 mol % DOPS, 3 mol % dansyl-PS, and 0.3 mol % NBD-PC in 10 mM Tris buffer (pH 7.0) displayed a random mixing of both NBD-PC (D, upper images) and dansyl-PS (same three vesicles, lower images). Addition of 20 μM unlabeled caveolin (82−101) induced the formation of dansyl-PS domains (E, lower images), but NBD-PC remained uniform (E, upper images). Similar results were obtained upon addition of 3 μM src (myr-2−19, C); NBD-PC was uniformly distributed in the vesicles (F, upper images), while domains enriched in dansyl-labeled PS were induced by the peptide. All images were normalized to a mean radiance value of 100 ± 5, and the corresponding intensity values are displayed using the pseudo-color scheme at the bottom of the figure. The white bar equals 4 μm.

appreciable signal in the dansyl channel of the fluorescence microscope (as in the bottom panel of Figure 8D). Figure 8C shows the same condition as in Figure 8B but with 3 μM src peptide added. The peptide induced the formation of NBS-PS domains; however, there was no dansyl fluorescence signal once again (as in the bottom panel of Figure 8D). Figure 8D shows the entire field of view for a large unilamellar vesicle of the same composition as in Figure 8B with 3 μM src peptide. The peptide induced the formation of a domain enriched in PS; however, the dansyl signal remained similar to background levels; there was no radiance value increase in the dansyl background fluorescence in these experiments (Figure 8D, lower panel). Thus, Figure 8D illustrates that the small, dansyl-labeled vesicles were not aggregating at the site of domain formation on the large unilamellar vesicle. Small vesicles have been added previously to large vesicles to label one leaflet of the bilayer (*59*). These experiments also showed the absence of aggregation and that the large vesicles were unilamellar.

Fluorescence Correlation Spectroscopy Experiments. The diffusion coefficients of an acrylodan-labeled N-terminal src peptide bound to the surface of large unilamellar vesicles were measured using two-photon excitation fluorescence correlation spectroscopy. This technique allows the selective excitation of fluorescent molecules in a small volume; fluorophores above and below the focal plane do not absorb photons (*53*). It is possible to obtain dynamic information about the rate at which molecules diffuse in to and out of the excitation volume and to calculate the number of molecules (on average) in that excitation volume. Figure 9 illustrates typical fluorescence correlation curves obtained from the autocorrelation function as described by Magde et al. (*60*) and Schwille et al. (*61*). Figure 9A shows the autocorrelation curve for the acrylodan-labeled src peptide diffusing free in solution at 269 $\mu m^2/s$. Upon addition of vesicles containing 33% acidic lipid, the N-terminal src peptide bound to the membrane surface diffused at 5.62 $\mu m^2/s$ (Figure 9B). Under the same conditions, on another vesicle, the acrylodan-labeled src peptide diffused at 1.23 $\mu m^2/s$ demonstrating a slower diffusion coefficient (Figure 9C). Figure 9D shows the autocorrelation curve for excitation of the sample background representing noise and cannot be fit to an autocorrelation function.

To gain insight into the lateral heterogeneity of the acrylodan-src peptide on the surface of vesicles containing acidic lipids, multiple regions on the same vesicle were excited, and the diffusion coefficients of the peptide in each region were calculated. A schematic representation of the vesicles and their excitation areas are shown in Figure 10. The vesicles in Figure 10A were composed of 90 mol %

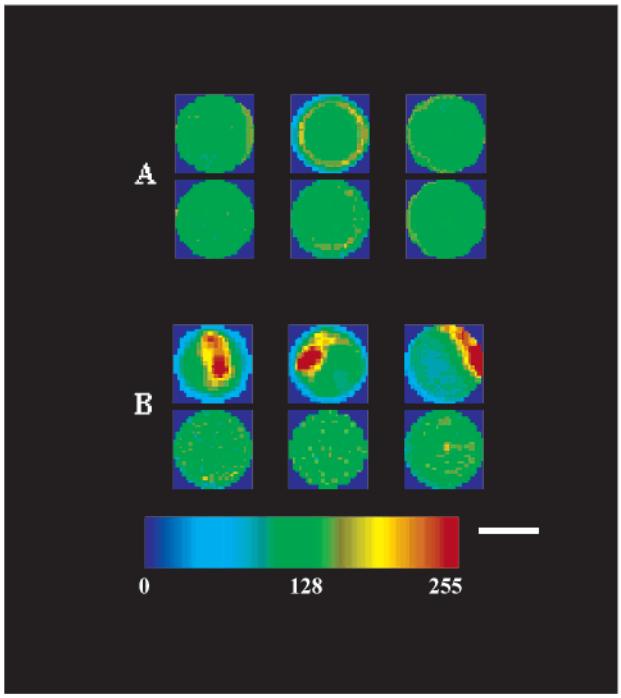

FIGURE 7: Gramicidin is not localized in membrane domains induced by the src peptide (myr-2−19, C). Vesicles composed of 67 mol % DOPC, 32.7 mol % DOPS, 0.3 mol % NBD-PS, and 20 μM dansyl-gramicidin were hydrated in 10 mM Tris buffer, pH 7.4 (A, upper images viewed for NBD-PS fluorescence and lower images are the same three vesicles viewed for dansyl-gramicidin fluorescence). There was a uniform distribution of PS and gramicidin in these vesicles. Membrane domains enriched in NBD-PS were formed in the presence of 3 μM src peptide (B, upper images). Dansyl-gramicidin remained uniform throughout the vesicles (B, lower images). All images were normalized to a mean radiance value of 100 ± 5, and the corresponding intensity values are displayed using the pseudo-color scheme at the bottom of the figure. The white bar equals 4 μm.

DOPC and 10 mol % DOPS with the addition of 0.05 μM acrylodan-labeled src peptide. A total of 10% acidic lipid was used in these experiments to minimize domain formation. The corresponding diffusion coefficients and the average number of molecules at each of the excitation regions are displayed below the vesicle. There was little heterogeneity in the diffusion rates or the average number of molecules in the excitation volume of the src peptide on the surface of the membrane in different vesicles or on the same vesicle. At this low concentration of peptide, domain formation was not visible. Figure 10B shows similar vesicles composed of 90 mol % DOPC and 10 mol % DOPS (left vesicle) and 67 mol % DOPC and 33 mol % DOPS (right vesicle) in the presence of 0.5 μM acrylodan-labeled src peptide and the corresponding excitation regions. There were marked differences in the diffusion rates of the src peptide between different areas on the same vesicle surfaces. As expected, there were a higher average number of src peptide molecules in the excitation region containing the slower diffusing peptide (Figure 10B). In vesicles composed of 67 mol % DOPC and 33 mol % DOPS in the presence of 3 μM acrylodan-labeled src peptide, there was a 2-fold difference in the diffusion rate of the membrane bound src peptide from region five of the vesicle versus region two of that same vesicle (Figure 10C). Also, there was a 2-fold difference in the average number of src peptide molecules between these regions; there were more src peptide molecules in the slower diffusing region of the vesicle membrane. Under the conditions shown in Figure 10B,C, acrylodan-labeled src peptide readily formed lateral membrane domains enriched in acidic lipids.

The error in measurement for the FCS data was calculated under conditions where no domains were present, specifically at low concentrations of src peptide (0.05 μM). In vesicles where domains did not form, there was a uniform distribution of src peptide on the membrane and diffusion rates and the number of molecules in the excitation volume when recorded at multiple points on the same vesicle. The calculated errors for the vesicles under the conditions of Figure 1 were 11.8% for the diffusion coefficients and 18.6% for the average concentration of molecules in the excitation volume. These error determinations cannot be performed on the measurements where domain formation was favorable as the diffusion coefficients and the number of molecules in the excitation volume varied greatly because of the nonrandom distribution of peptides bound to the vesicles. The errors calculated under conditions where no domains were present should be applicable for all measurements even when domains were present since all experiments were performed in the same manner.

Sources of error in these FCS measurements lie in the signal-to-noise ratio of the diffusing, fluorescent peptide; too much peptide in the excitation volume decreases the sensitivity of the discriminator to identify diffusing molecules. Similarly, these measurements depend on the laser power and the width of the excitation volume (typically 0.30 × 0.30 μm). Another source of error lies in focusing the laser directly at the membrane surface because the signal decreased dramatically above and below the membrane. The error in measuring the diffusion rates also depends on the frequency of counting the emitted photons; the data presented here were recorded at 20 kHz and allowed for monitoring the diffusing peptide on the membrane surface. It was not possible to visualize the fluorescence emission and therefore the location of domains in the vesicles, so the data reflect random excitation points taken on the vesicle surface. Some points would be expected to reflect regions with no domains, and some points would reflect regions with domains or most likely regions with partial domains. The large differences in the diffusion coefficients found at the higher concentration of src peptide are consistent with this interpretation. The results also indicate that domains are dynamic with considerable, albeit slower, diffusion.

DISCUSSION

Membrane domains present a new level of molecular organization that allows the regulation and an increase in specificity for the interactions of membrane bound cell signaling components. The experiments in this paper show that the membrane binding regions of src and caveolin bound to and localized into lateral membrane domains enriched in acidic lipids. The caveolin scaffolding domain (residues 82−101) also sequestered cholesterol into these domains. The colocalization of caveolin and src peptides into the membrane domains resulted in the inhibition of PKC phosphorylation of src. It was also recently shown that NAP-22, a major component of neuronal rafts, can induce the formation of cholesterol-rich domains (*43*). Protein-induced domains

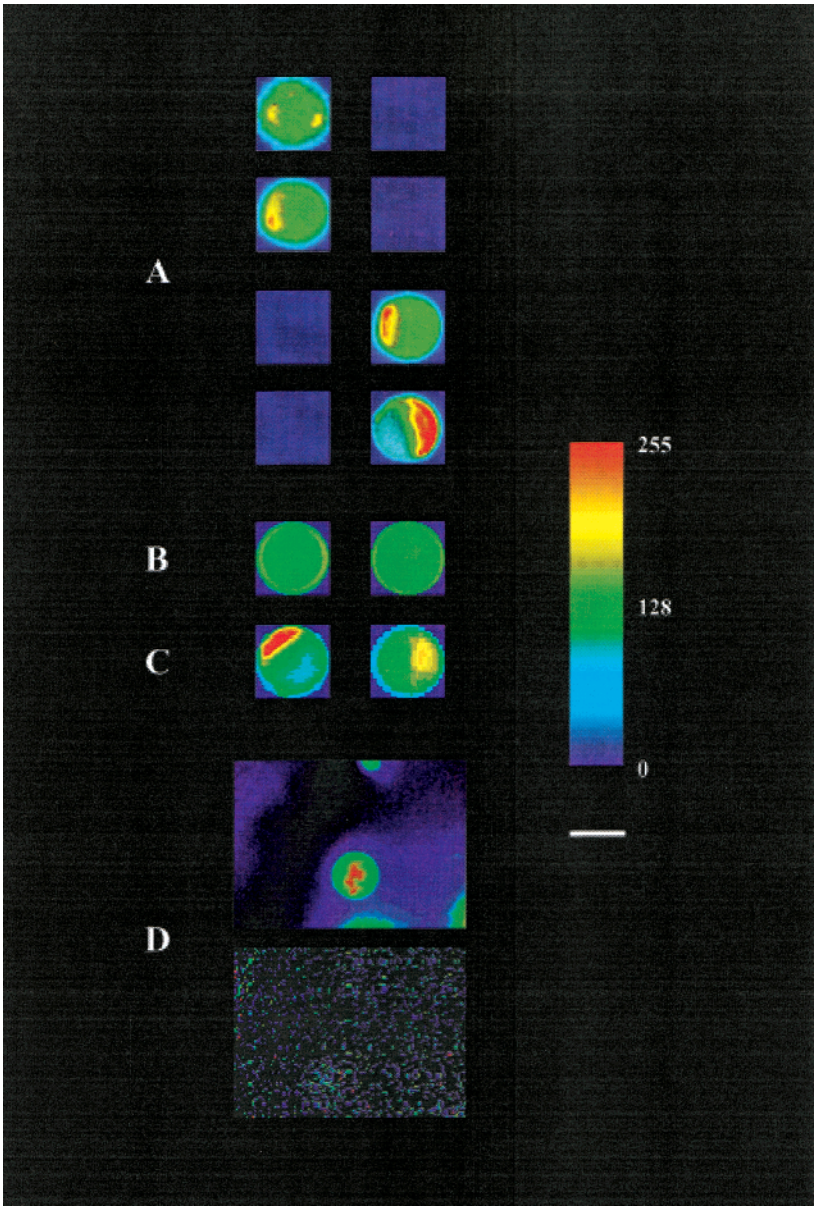

FIGURE 8: Formation of lateral membrane domains enriched in PS induced by the src peptide (myr-2−19, C) in the presence of large and small vesicles labeled with another fluorophore do not show aggregation. The vesicles shown in A were taken from an equimolar mixture of large unilamellar vesicles composed of 67 mol % DOPC, 32.7 mol % DOPS, and 0.3 mol % NBD-PS for one type of vesicle and 67 mol % DOPC, 30 mol % DOPS, and 3 mol % dansyl-PS for the other type of vesicle in 10 mM Tris buffer, pH 7.4. The images on the left were viewed for dansyl-PS fluorescence, and the images on the right show the corresponding images of the same vesicles but viewed for NBD-PS. The vesicles showing dansyl-PS enriched domains (top two vesicles) did not show any NBD fluorescence above background. Conversely, vesicles showing NBD-PS domains (bottom two vesicles) did not show any dansyl fluorescence. In B, large unilamellar vesicles labeled with NBD-PS (as in A) were mixed with dansyl-labeled small, extruded vesicles (67 mol % DOPC, 30 mol % DOPS, and 3 mol % dansyl-PS, 100 nm, 0.1 mM final concentration). Without the src peptide there was a uniform distribution of PS in the vesicles. There was no significant fluorescence signal upon excitation of the dansyl-labeled extruded vesicles (as in the bottom of D, not shown). C shows vesicles as in B with 3 μM unlabeled src peptide (myr-2−19, C) added. Images reflect NBD-PS fluorescence demonstrating the formation of membrane domains enriched in PS induced by the src peptide. There was no significant fluorescence signal upon excitation of the dansyl-labeled extruded vesicles (as in the bottom of D, not shown). D shows a full-field view of a vesicle under the same conditions as in C. The upper image is viewed for NBD-PS fluorescence, while the lower panel is the same field viewed for dansyl-PS fluorescence. The white bar equals 4 μm.

may explain the localization of many signaling molecules in caveolae and may shed light on how caveolar localization of signaling molecules renders proteins inactive, referred to as the caveolin signaling hypothesis (*62*). Changing the properties of proteins by phosphorylation or other means may result in rearrangement of the domains or the partitioning of molecules into or out of a domain. The changes in the domains would not have to rely on the properties of a liquid-ordered phase.

Although there is controversy in how caveolin binds to membranes, it is becoming clear that residues 82−101 play a critical role in the protein's function. The caveolin scaffolding region is vital for binding to the plasma membrane (*27*). Fluorescence digital imaging microscopy experiments here showed that caveolin (82−101) induced the formation of domains enriched in PS, PIP_2, and cholesterol. Arbuzova et al. (*63*) studied the caveolin peptide 92−100 and found that the aromatic residues anchored the peptide weakly to

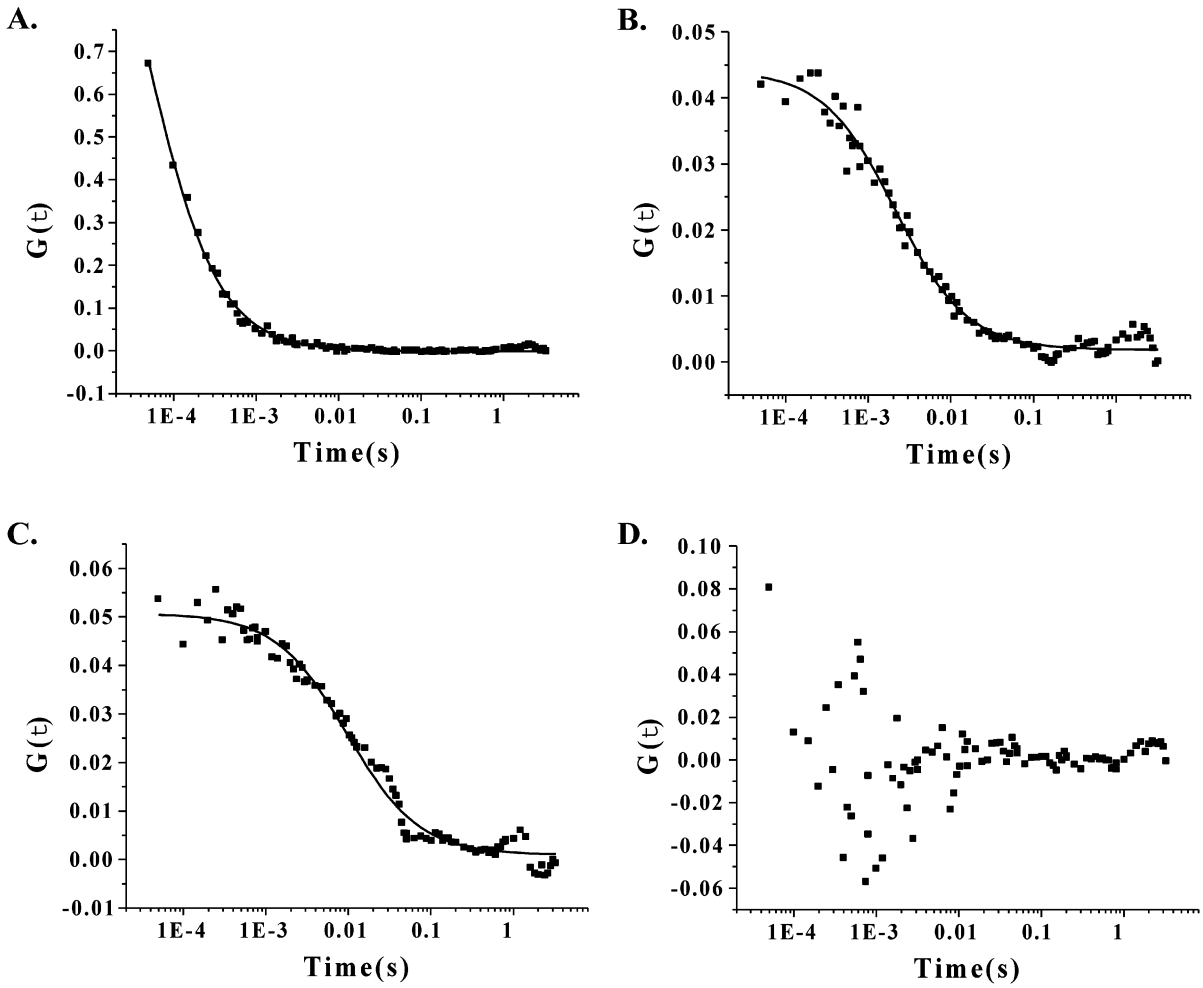

FIGURE 9: Two-photon excitation fluorescence correlation spectroscopy curves of an acrylodan-labeled src peptide (acr-myr-2−19, C) on the surface of vesicles. Graph A depicts the autocorrelation curve of acrylodan-labeled src peptide diffusing in 0.5 mM MOPS buffer, pH 7.4. Large unilamellar vesicles containing 67 mol % DOPC and 33 mol % DOPS were incubated with the 3 μM acrylodan-labeled src peptide, and FCS measurements were taken with the focus on the surface of the vesicle (B). Graph C shows the same analysis of another vesicle at the same condition as in B. Graph D illustrates FCS measurements focusing on the background. Black squares indicate data points, and the curves represent the 2D Gaussian fit performed using PV-WAVE (Visual Numerics) and Origin (Microcal Software, Inc.) software.

the membrane and that the basic residues caused a larger enhancement of binding. Schlegel and Lisanti (*64*) studied the membrane binding characteristics of deletion mutants of caveolin. These authors discovered that caveolin mutants missing the membrane spanning region (residues 102−134) bound to the membrane and still targeted to caveolae (*64*). The authors hypothesized that there may be two targeting signals for caveolin membrane binding and that the scaffolding region (82−101) was critical for rendering localization and holding other signaling molecules in inactive states (*64*). Furthermore, the authors suggested that caveolin cycles between different phosphorylation states and that this alters caveolin localization and hence function (*64*). The results of this study correlate well with the notion of protein-induced membrane domains similar to domains formed by MARCKS (myristoylated alanine-rich C kinase substrate) in the calcium−phospholipid second messenger system (*1*, *2*). MARCKS forms domains enriched in acidic lipids PS and PIP_2. In the presence of calcium and diacylglycerol, the concentration of the activators of PKC in the domains, along with the substrate MARCKS, causes PKC to phosphorylate MARCKS at an increased rate (*1*). Phospholipase C, on the other hand, is not enriched in the domains, and this results in an inhibition of phospholipase C activity. The basis of the inhibition lies in the spatial separation of enzyme (PLC) and substrate (PIP_2) (*2*). PKC phosphorylation of MARCKS altered its membrane binding characteristics and released the inhibition of PLC (*2*). Thus, lateral membrane domain formation has been shown to affect the function of enzymes in signaling cascades. Caveolin may act in a manner similar to MARCKS by sequestering proteins and/or lipids into domains and changing their activity.

The mechanism of lipid sequestration induced by the caveolin scaffolding region probably is similar to that of the MARCKS membrane binding region and primarily involves the nonspecific electrostatic attraction of basic residues of the protein with acidic lipids in the membrane. In addition, hydrophobic residues contribute to membrane binding; however, the effect of these amino acids on domain formation is not well-characterized. A recent EPR has shown that the MARCKS peptide sequesters multiple PIP2 molecules within the plane of the membrane (*65*), which is consistent with the observation of domain formation induced by the MARCKS peptide using fluorescence digital imaging microscopy (*2*, *7*). Another signaling molecule, src has a similar membrane binding motif; src binds to the plasma membrane via insertion

A

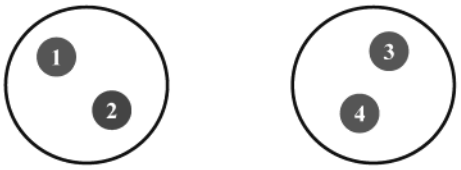

Excitation Area	D (μm²/s)	Number of Molecules
1	17.0 +/- 1.99	0.54 +/- 0.099
2	18.0 +/- 2.11	0.32 +/- 0.059
3	16.0 +/- 1.87	0.39 +/- 0.073
4	16.4 +/- 1.92	0.31 +/- 0.058

B

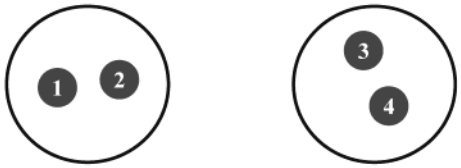

Excitation Area	D (μm²/s)	Number of Molecules
1	1.91	1.53
2	12.6	0.72
3	2.39	1.56
4	11.3	0.47

C

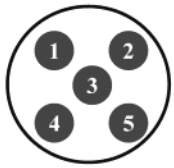

Excitation Area	D (μm²/s)	Number of Molecules
1	10.3	6.83
2	14.6	6.29
3	10.5	7.83
4	9.86	10.0
5	7.44	12.6

FIGURE 10: Two-photon excitation FCS data of an acrylodan-labeled src peptide (myr-2−19, C) bound to the surface of vesicles. The schematic vesicles in A show the areas of two-photon excitation on the surface of each vesicle (composed of 90 mol % DOPC and 10 mol % DOPS) in the presence of 0.05 mM acrylodan-labeled src peptide (numbered dots). The corresponding diffusion coefficients and number of molecules in the excitation volume at each excitation point are shown below the vesicles. (The numbers of molecules are in units of nM since they are relative to a standard solution of 5 nM rhodamine free in solution even though src was bound to the membrane, that is, in two dimensions. The true excitation volume cannot be directly measured.) Under these conditions, there was a uniform diffusion coefficient and average number of molecules in the excitation volume between vesicles and within the same vesicle. B shows similar vesicles composed of 90 mol % DOPC and 10 mol % DOPS (left) and 67 mol % DOPC and 33 mol % DOPS (right) in the presence of 0.5 mM acrylodan-labeled src peptide and the corresponding two-photon excitation points. There were significant differences in the diffusion coefficients and the average number of molecules on the surface of the same vesicle in each condition, indicating a heterogeneous distribution of peptide bound to the surface of the membrane. C shows a vesicle composed of 67 mol % DOPC and 33 mol % DOPS in the presence of 3 mM acrylodan-labeled src (myr-2−19, C). This vesicle was excited at five different areas and shows a heterogeneous distribution of peptide bound to the surface and a corresponding difference in the diffusion rates in areas of the same vesicle. Error of measurement was determined under conditions where membrane domains of the src peptide did not form. Multiple vesicles were excited at different places on their surfaces, and a percent error was calculated for both the diffusion coefficient and the average concentration of molecules in the excitation volume.

of a N-terminal myristate chain and a cluster of basic residues just downstream of the lipid anchor (*30*). The membrane binding region of src (myr-2−19, C) was shown to be localized into domains enriched in acidic lipids along with the caveolin scaffolding domain. Both the acidic lipids and the src peptide were highly enriched in domains under physiological conditions.

The caveolin scaffolding region is thought to be important for oligomerization with other caveolin molecules and as well as in interacting with other proteins (*26*). A recent model suggests that the caveolin (79−96) peptide is helical and interacts laterally to form the heptameric subunits that then form the filamentous coat of caveolae (*66*). If the peptide is involved in protein−protein interactions, it does not preclude its interactions with lipids. The main driving force of membrane domain formation (i.e., caveolae formation) could be the protein−protein interactions, and the interactions with lipids could result in specific lipids being sequestered into the domains.

Phosphorylation of the N-terminal membrane binding region of src is thought to cause its translocation from the plasma membrane in response to growth factors (*33*). This phosphorylation has been shown to enhance src activity (*67*). Oka et al. (*68*) demonstrated that caveolin interacts with PKC and inhibits PKC phosphorylation of peptides corresponding to myelin basic protein in a dose-dependent manner. They further showed that the scaffolding region of caveolin was responsible for this inhibition (*68*). In this report, we showed that PKC phosphorylation of the src peptide (myr-2−19, C) was inhibited by the caveolin scaffolding region. Increasing concentrations of caveolin (82−101) peptide inhibited the PKC phosphorylation of src (myr-2−19, C). One explanation for the basis of this inhibition lies in the colocalization of caveolin (82−101) and src (myr-2−19, C) in lateral membrane domains. The N-terminal membrane binding region of src contains phosphorylation sites for protein kinase C and protein kinase A. The function of N-terminal src phosphorylation is not well-understood; however, the phosphorylation event may serve to activate src (*31*). Src tyrosine kinase has been shown to phosphorylate the caveolin protein on its N-terminus both *in vitro* and *in vivo* (*69*). PKC or PKA phosphorylation of src may lead to its activation and subsequent phosphorylation of src substrates, one of which is the N-terminus of caveolin. Introducing negatively charged phosphates into caveolin may decrease its affinity for domains, thereby activating cell signaling. Having src and caveolin localized into membrane domains can account for this additional level of regulation of cell signaling, although the molecular mechanism of how caveolin inhibits PKC activity remains unclear.

Murray et al. (*58*) have raised a question as to whether the domains induced by basic peptides that are observed by fluorescence microscopy are due to true domain formation. They suggest the domains that are observed may be due to aggregation of vesicles, probably followed by collapse/explosion of the secondary vesicles onto the surface of the primary vesicles. These authors mention four experimental observations. First, when domains are observed by fluorescence microscopy, there is a colocalized area of extra darkness when observed by phase contrast microscopy. Second, when using acrylodan-labeled peptides, the increase in NBD-PS (or bodipy-PS) in domains is the same as the

increase in NBD-PC (or bodipy-PC) in domains rather than a decrease in NBD-PC (or bodipy-PC). Third, no detectable peptide-induced domains were observed in monolayers. Fourth, the MARCKS peptide inhibited phospholipase C hydrolysis of PIP_2 (*2*). This was originally explained as because of MARCKS-induced formation of domains enriched in PIP_2 as observed by fluorescence microscopy and phospholipase C being excluded from the domains. Murray et al. (*58*) suggest the inhibition of phospholipase C is readily explained by vesicle aggregation.

These observations can be explained by mechanisms other than vesicle aggregation. It should be noted that the putative vesicle aggregation giving rise to domains discussed by Murray et al. (*58*) is hypothetical and it is not observed in the vesicles whose images are collected for fluorescence microscopy. While a small fraction of the vesicles do aggregate or touch each other under our experimental conditions, this is easily observed by direct microscopic observation since the vesicles are large. The vesicles are always examined to be sure that they are single vesicles with no signs of aggregation before images of the vesicles are captured. Murray et al. (*58*) acknowledge that simple aggregation is not what occurs, and they suggest instead vesicle aggregation probably followed by collapse/explosion of the secondary vesicles onto the surface of the primary vesicle. If there was a substantial amount of vesicle collapse/aggregation that occurred, it seems that there should be some intermediate structures visible. That is, there should be many domains with collapsed vesicles or small, but visible, vesicles adhering to the domains. This is not observed by direct microscopic observation. It should also be noted that the domains we observe that are induced by basic peptides are substantially enriched in both acidic lipids and peptides. In the experiments reported in this paper, the range of lipid concentrations in vesicles caused by the peptides is 4−7-fold. Substantial aggregation would have to occur to obtain these enrichments and that should be readily observed under the microscope. We arbitrarily define a domain as having an enrichment greater than 1.5−2-fold the average radiance value of the vesicle. This was initially done because early CCD cameras had a high noise level, but this definition has been maintained, and it also serves to eliminate minor aggregation even if it is not visible. In addition, a population of vesicles is always examined rather than relying on the results from a single vesicle.

To directly address the points raised by Murray et al. (*58*): First, aggregation is not observed by either phase contrast microscopy (with white light) in the domains or with fluorescence microscopy. Darkness with phase contrast could be due to a number of factors. There is a significantly higher concentration of peptide and fluorophores in the domains. This should give rise to a difference in refractive index that may be detected by phase contrast. Also, the increase in the concentration of the peptide and fluorophores in the domains could lead to higher absorption of light. Photobleaching does not remove material and/or it may not completely destroy all chromophores. Also, the domains could have an irregular surface (even if it is not visible) that could appear as darkness. Second, using high concentrations of fluorophores, as done by Murray et al. (*58*), can lead to energy transfer between acrylodan and both NBD and bodipy. Domains enriched in PS still contain PC, and not all the peptide is in the domains. Consequently, some energy transfer can take place with both NBD and bodipy. If the microscope filters are broad, which they usually are, then energy transfer can readily be observed. Without careful quantitation, it cannot be determined if the signal from PS fluorescence is similar to PC fluorescence. When better choices are used for the fluorescence pair (e.g., NBD- and dansyl-labeled lipids) and the proper filters are used, PC is not enriched in the domains as shown in this paper and in previous papers (*7*, *56*, *57*). Third, monolayers are quite different from bilayers, and if domains are not observed in monolayers it may mean that there are different forces and packing in monolayers to account for the different results. Fourth, vesicle aggregation could account for the inhibition of phospholipase C activity by the MARCKS peptide. However, in a subsequent paper the same group concludes that the reversible inhibition of phospholipase C by the MARCKS peptide is not the result of peptide-induced vesicle aggregation (*70*). If secondary vesicles had collapsed or exploded on the surface of the large vesicles, it is unlikely that it would be readily reversible. Phosphorylation of the MARCKS peptide by protein kinase C caused the peptide to come off the vesicle and reversed domain formation (*1*). Calcium/calmodulin also rapidly removes the MARCKS peptide from vesicles, and it approaches a diffusion-limited rate (*71*). If vesicle aggregation does not account for the phospholipase C inhibition, it seems vesicle aggregation may not account for the fluorescence microscopy results either. It should also be noted that the MARCKS peptide-induced domains lead to the activation of protein kinase C rather than the inhibition of the protein kinase C (*1*, *7*). This occurs over a wide range of peptide concentrations.

In addition to observing the vesicles visually, a number of control experiments were carried out to rule out that the domains were due to aggregation and/or collapse/explosion of vesicles: (1) Not all lipids (and proteins) are enriched in the domains. Double-labeling experiments show that PC and gramicidin are not enriched in the domains. If aggregation were taking place, similar enrichments should be observed. (2) Large and small vesicles labeled with a different fluorophore do not aggregate with the large vesicles when peptides are added to induce domain formation. (3) Fluorescence energy transfer experiments using calcium and other proteins, a second independent technique, give results that support the domain formation observed by fluorescence digital imaging microscopy (*56*, *57*, *59*, *72*). (4) The total fluorescence intensity of PS or other labeled lipids in the vesicles observed by fluorescence microscopy does not increase when the peptide is added. If vesicles were aggregating with the large vesicle, the overall vesicle fluorescence should increase. (5) A theoretical explanation has been given for basic peptide-induced domain formation that explains, for example, the experimental observation that domains form at low concentrations of pentalysine but do not form at high concentrations of pentalysine (*3*). This behavior is not consistent with the mechanism of vesicle aggregation being responsible for domain formation. While it is possible that a small amount of vesicle aggregation may occur, these results rule out that the contribution is significant.

Further illustrating the heterogeneity of lipids and peptides in membranes, FCS measurements showed distinct differences in the diffusion rates of an acrylodan-labeled src peptide bound to the vesicle surface. Under conditions where

the N-terminal src peptide induced the formation of membrane domains, there were differences in the diffusion rates of src not only bound to different vesicles at the same condition but differences in the diffusion rates upon excitation of different areas on the same vesicle surface. Thus, while the overall shape of the domains may not change when viewed for a couple of minutes (fluorescence microscopy images), the domains seem to be very dynamic, possibly reflecting rapid association and dissociation events. Further work using this sensitive technique may shed light on the mechanism of protein-induced membrane domain formation. The membrane domain formation induced by the caveolin scaffolding region and src provides insight into how the membrane can organize signaling lipids and proteins. This organization at the membrane level can help explain the specific regulation and cross-talk, or lack of cross-talk, of signal transduction pathways.

ACKNOWLEDGMENT

We thank John Eid and Dr. Theodore Hazlett (Laboratory for Fluorescence Dynamics, University of Illinois, Urbana, IL) for help with the two-photon excitation fluorescence correlation spectroscopy experiments.

REFERENCES

1. Yang, L., and Glaser, M. (1995) *Biochemistry 34*, 1500−1506.
2. Glaser, M., Wanaski, S., Buser, C. A., Boguslavsky, V., Rashidzada, W., Morris, A., Rebecchi, M., Scarlata, S. F., Runnels, L. W., Prestwich, G. D., Chen, J., Aderem, A., Ahn, J., and McLaughlin, S. (1996) *J. Biol. Chem. 271*, 26187−26193.
3. Denisov, G., Wanaski, S., Luan, P., Glaser, M., and McLaughlin, S. (1998) *Biophys. J. 74*, 731−744.
4. Rogers, W., and Glaser, M. (1993a) *Biochemistry 32*, 12591−12598.
5. Rogers, W., and Glaser, M. (1993b) in *Optical Microscopy: New Technologies and Applications* (Herman, B., and Lemasters, J., Eds.) pp 263−283, Academic Press, San Diego, CA.
6. Luan, P., and Glaser, M. (1994) *Biochemistry 33*, 4483−4489.
7. Yang, L., and Glaser, M. (1996) *Biochemistry 35*, 13966−13974.
8. Anderson, R. G. W. (1993) *Proc. Natl. Acad. Sci. U.S.A. 90*, 10909−10913.
9. Parton, R. G. (1996) *Curr. Opin. Cell Biol. 8*, 542−548.
10. Schlegel, A., Volonte, D., Engelman, J. A., Galbiati, F., Mehta, P., Zhang, X. L., Scherer, P. E., and Lisanti, M. P. (1998) *Cell. Signalling 10*, 457−463.
11. Okamoto, T., Schlegel, A., Scherer, P. E., and Lisanti, M. P. (1998) *J. Biol. Chem. 273*, 5419−5422.
12. Oh, P., McIntosh, D. P., and Schnitzer, J. E. (1998) *J. Cell Biol. 141*, 101−114.
13. Henley, J. R., Krueger, E. W., Oswald, B. J., and McNiven, M. A. (1998) *J. Cell Biol. 141*, 85−99.
14. Smart, E. J., Ying, Y.-S., and Anderson, R. G. (1995) *J. Cell Biol. 131*, 929−938.
15. Liu, J., Oh, P., Horner, T., Rogers, R. A., and Schnitzer, J. E. (1997) *J. Biol. Chem. 272*, 7211−7222.
16. Pike, L. J., and Casey, L. (1996) *J. Biol. Chem. 271*, 26453−26456.
17. Liu, P., and Anderson, R. G. (1995) *J. Biol. Chem. 270*, 27179−27185.
18. Smart, E. J., Ying, Y.-S., Donzell, W. C., and Anderson, R. G. W. (1996) *J. Biol. Chem. 271*, 29427−29435.
19. Sargiacomo, M., Sudol, M., Tang, Z.-L., and Lisanti, M. P. (1993) *J. Cell Biol. 122*, 789−807.
20. Jacobson, K., and Dietrich, C. (1999) *Trends Cell Biol. 9*, 87−91.
21. London, E., and Brown, D. A. (2000) *Biochim. Biophys. Acta 1508*, 182−195.
22. Simons, K., and Ikonen, E. (1997) *Nature 387*, 569−572.
23. Dobrowsky, R. T. (2000) *Cell. Signalling 12*, 81−90.
24. Rothberg, K. G., Heuser, J. E., Donzell, W. C., Ying, Y.-S., Glenney, J. R., and Anderson, R. G. W. (1992) *Cell 68*, 673−682.
25. Monier, S., Parton, R. G., Vogel, F., Behlke, J., Henske, A., and Kurzchalia, T. V. (1995) *Mol. Biol. Cell 6*, 911−927.
26. Sargiacomo, M., Scherer, P. E., Tang, Z.-L., Kubler, E., Song, K. S., Sanders, M. C., and Lisanti, M. P. (1995) *Proc. Natl. Acad. Sci. U.S.A. 92*, 9407−9411.
27. Schlegel, A., Schwab, R. B., Scherer, P. E., and Lisanti, M. P. (1999) *J. Biol. Chem. 274*, 22660−22667.
28. Ben-Tal, N., Honig, B., Peitzsch, R. M., Denisov, G., and McLaughlin, S. (1996) *Biophys. J. 71*, 561−575.
29. Wimley, W. C., and White, S. H. (1996) *Nature Struct. Biol. 3*, 842−848.
30. Buser, C. A., Sigal, C. T., Resh, M. D., and McLaughlin, S. (1994) *Biochemistry 33*, 13093−13101.
31. Gould, K. L., Woodgett, J. R., Cooper, J. A., Buss, J. E., Shalloway, D., and Hunter, T. (1985) *Cell 42*, 849−857.
32. Murray, D., Hermida-Matsumoto, L., Buser, C. A., Tsang, J., Sigal, C. T., Ben-Tal, N., Honig, B., Resh, M. D., and McLaughlin, S. (1998) *Biochemistry 37*, 2145−2159.
33. Oude Weernink, P. A., and Rijksen, G. (1995) *J. Biol. Chem. 270*, 2264−2267.
34. Walker, F., deBlaquiere, J., and Burgess, A. W. (1993) *J. Biol. Chem. 268*, 19552−19558.
35. Bradley, A. J., Maurer-Spurej, E., Brooks, D. E., and Devine, D. V. (1999) *Biochemistry 38*, 8112−8123.
36. May, S., Harries, D., and Ben-Shaul, A. (2000) *Biophys. J. 79*, 1747−1760.
37. Heimburg, T., Angerstein, B., and Marsh, D. (1999) *Biophys. J. 76*, 2575−2586.
38. Gil, T., Ipsen, J. H., Mouritsen, O. G., Sabra, M. C., Sperotto, M. M., and Zuckermann, M. J. (1998) *Biochim. Biophys. Acta 1376*, 245−266.
39. Sabra, M. C., Uitdehaag, J. C. M., and Watts, A. (1998) *Biophys. J. 75*, 1180−1188.
40. Maierhofer, A. P., Bucknall, D. G., and Bayerl, T. M. (2000) *Biophys. J. 79*, 1428−1437.
41. Polozova, A., and Litman, B. J. (2000) *Biophys. J. 79*, 2632−2643.
42. Hinterliter, A., Almeida, P. F. F., Creutz, C. E., and Biltonen, R. L. (2001) *Biochemistry 40*, 4181−4191.
43. Epand, M. E., Maekawa, S., Yip, C. M., and Epand, R. F. (2001) *Biochemistry 40*, 10514−10521.
44. Haverstick, D. M., and Glaser, M. (1987) *Proc. Natl. Acad. Sci. U.S.A. 84*, 4475−4479.
45. Needham, D., and Evans, E. (1988) *Biochemistry 27*, 8261−8269.
46. Gupta, C. M., Radhakrishnan, R., and Khorana, H. G. (1977) *Proc. Natl. Acad. Sci. U.S.A. 74*, 4315−4319.
47. Bligh, E. G., and Dyer, W. J. (1959) *Can. J. Biochem. Physiol. 37*, 911−917.
48. Kates, M. (1972) in *Techniques in Lipidology*, pp 335−336, American Elgevire, New York.
49. Comfurious, P., Bevers, E. M., and Zwaal, R. F. A. (1990) *J. Lipid Res. 31*, 1719−1921.
50. Stabel, S., Schaap, D., and Parker, P. (1991) *Methods Enzymol. 200*, 670−673.
51. Chakravarthy, B. R., Bussey, A., Whitfield, J. F., Sikorska, M., Williams, R. E., and Durkin, J. P. (1991) *Analytical Biochem. 196*, 144−150.
52. Edashige, K., Utsumi, T., Sato, E. F., Ide, A., Kasai, M., and Utsumi, K. (1992) *Archives of Biochem. Biophys. 296*, 296−301.
53. Bagatolli, L. A., and Gratton, E. (2000) *Biophys. J. 78*, 290−305.
54. Chen, Y., Muller, J. D., So, P. T. C., and Gratton, E. (1999) *Biophys. J. 77*, 553−567.
55. Gilmore, R., Cohn, N., and Glaser, M. (1979) *Biochemistry 18*, 1042−1049.
56. Luan, P., Yang, L., and Glaser, M. (1995) *Biochemistry 34*, 9874−9883.
57. Haverstick, D. M., and Glaser, M. (1989) *Biophys. J. 55*, 677−682.
58. Murray, D., Arbuzova, A., Hangyas-Mihalyne, G., Gambhir, A., Ben-Tal, N., Honig, B., and McLaughlin, S. (1999) *Biophys. J. 77*, 3176−3188.
59. Haverstick, D. M., and Glaser, M. (1988) *J. Cell Biol. 106*, 1885−1892.

60. Magde, D., Elson, E., and Webb, W. W. (1972) *Phys. Rev. Lett. 29*, 705−708.
61. Schwille, P., Korlach, J., and Webb, W. W. (1999) *Cytometry 36*, 176−182.
62. Razani, B., Schlegel, A., and Lisanti, M. P. (2000) *J. Cell Sci. 113*, 2103−2109.
63. Arbuzova, A., Wang, L., Wang, J., Hangyas-Mihalyne, G., Murray, D., Honig, B., and McLaughlin, S. (2000) *Biochemistry 39*, 10330−10339.
64. Schlegel, A., and Lisanti, M. P. (2000) *J. Biol. Chem. 275*, 21605−21617.
65. Rauch, M. E., Ferguson, C. G., Prestwich, G. D., and Cafiso, D. S. (2002) *J. Biol. Chem. 277*, 14068−14076.
66. Fernandez, I., Ying, Y., Albanesi, J., and Anderson, R. G. W. (2002) *Proc. Natl. Acad. Sci. U.S.A. 99*, 11193−11198.
67. Liebenhoff, U., Brockmeier, D., and Presek, P. (1993) *Biochem. J. 295*, 41−48.
68. Oka, N., Yamamoto, M., Schwencke, C., Kawabe, J., Ebina, T., Ohno, S., Couet, J., Lisanti, M. P., and Ishikawa, Y. (1997) *J. Biol. Chem. 272*, 33416−33421.
69. Li, S., Seitz, R., and Lisanti, M. P. (1996) *J. Biol. Chem. 271*, 3863−3868.
70. Wang, J., Arbuzova, A., Hangyas-Mihalyne, G., and McLaughlin, S. (2001) *J. Biol. Chem. 276*, 5012−5019.
71. Arbuzova, A., Murray, D., and McLaughlin, S. (1998) *Biochim. Biophys. Acta 1376*, 369−379.
72. Wang, S., Martin, E., Cimino, J., Omann, G., and Glaser, M. (1988) *Biochemistry 27*, 2033−2039.

BI012097N